

Piecewise mass flows within a solar prominence observed by the New Vacuum Solar Telescope

Hongbo Li^{1,2,3}  · Yu Liu^{1,2} · Kuan Vai Tam⁴ · Mingyu Zhao¹ · Xuefei Zhang¹

Received: 15 December 2017 / Accepted: 8 May 2018 / Published online: 16 May 2018
© Springer Science+Business Media B.V., part of Springer Nature 2018

Abstract The material of solar prominences is often observed in a state of flowing. These mass flows (MF) are important and useful for us to understand the internal structure and dynamics of prominences. In this paper, we present a high resolution H α observation of MFs within a quiescent solar prominence. From the observation, we find that the plasma primarily has a circular motion and a downward motion separately in the middle section and legs of the prominence, which creates a piecewise mass flow along the observed prominence. Moreover, the observation also shows a clear displacement of MF's velocity peaks in the middle section of the prominence. All of these provide us with a detailed record of MFs within a solar prominence and show a new approach to detecting the physical properties of prominence.

Keywords Sun: activity · Sun: filaments, prominences · Sun: magnetic fields

1 Introduction

Solar prominences are one of the most common magnetic structures on the solar atmosphere (Hirayama 1985; Mar-

tin 1998; Mackay et al. 2010). They are embedded in the tenuous corona and usually possess some legs extending to the photosphere (Martin 1998; Liu and Kurokawa 2004; Parenti 2014; Su et al. 2015). Although they often keep a certain shape for a long period, the internal material of them is highly dynamic (Berger et al. 2008; Ning et al. 2009; Lin 2011; Parenti 2014; Su et al. 2015). Many observations indicate that the material can move synchronically and develop into mass flows (MFs) in some prominences (Zirker et al. 1998; Lin et al. 2003, 2005). These MFs are closely related to the dynamic equilibrium of prominence (Schmieder et al. 2010, 2015; Yan et al. 2015; Okamoto et al. 2016). However, further details about these MFs and their relationship with the magnetic field of prominence have not yet been well understood (Parenti 2014).

In this work, we present a comprehensive analysis about the MFs in a quiescent prominence observed by the New Vacuum Solar Telescope (NVST) on 2016 November 5. It reveals that there are primarily two types of MF existing in the middle section and leg of the prominence, respectively. Other observational characteristics of the prominence have also been discussed. By combining these characteristics, we suggest that the observed different MFs may be caused by the different physical conditions and particular magnetic topological structure of the prominence. All these investigations show us a more completed physical image of MFs within a quiescent solar prominence that significantly improves our knowledge on prominence MFs and provides some new clues for the further study on the internal structure and dynamics of solar prominence.

2 Observation and methods

The prominence under study was recorded on a sequence of H α (6563 Å) images by the New Vacuum solar Telescope

✉ H. Li
hbli@ynao.ac.cn

¹ Yunnan Observatories, Chinese Academy of Sciences, Kunming 650011, China

² Key Laboratory of Geospace Environment, Chinese Academy of Sciences, University of Science & Technology of China, Hefei 230026, China

³ University of Chinese Academy of Sciences, Beijing 100049, China

⁴ Space Science Institute, Macau University of Science and Technology, Avenida Wai Long, Taipa, Macau, China

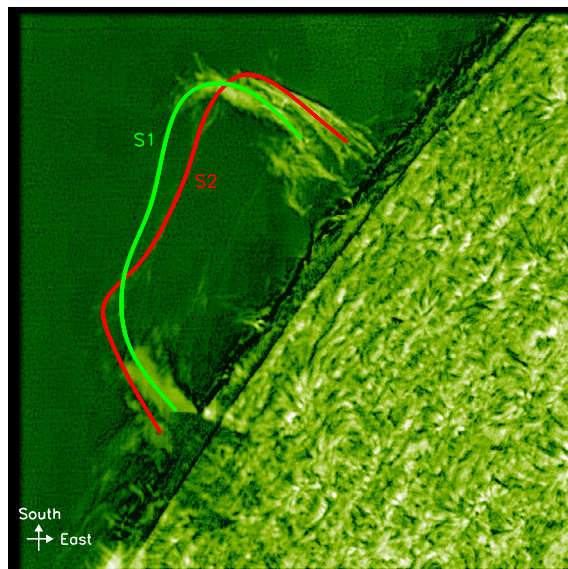


Fig. 1 An overview of the prominence observed by NVST on the $H\alpha$ channel. The two branches of the prominence are indicated by the green (S1) and red (S2) thick lines

(NVST; Liu et al. 2014b), which is operated by Yunnan Observatories, Chinese Academy of Sciences. The images were taken at the $H\alpha$ line core obtained by using a tunable Lyot filter with a bandwidth of 0.25 \AA . The observation lasted from 03:40 UT to 06:06 UT on 2016 November 5. In order to correct the blurring effect of the turbulent atmosphere on earth, a series of speckle reconstruction techniques have been used to reconstruct the high resolution images from the raw data (Xiang et al. 2016). The reconstructed images cover a $168'' \times 168''$ field of view and have a spatial resolution of $0.164''$ and a temporal cadence of 11 s.

The prominence was located on the southwest limb of the sun, within which the material flowed and outlined the two main entwined branches of prominence. Based on the trajectories of these MFs, we picked the two branches (S1 and S2) manually. An overview of the prominence is shown in Fig. 1, where the two branches are marked by the green (S1) and red (S2) thick lines, along with which two time-distance maps (Fig. 2 and Fig. 3) were interpolated by applying the bilinear interpolation. From these maps, different types of MFs can be identified. To analyze the MFs quantitatively, two main steps were used to extract the MFs. On the first step, we needed to outline the MFs and interpolated them into rough tracks by the cubic spline interpolation. Secondly, we took the brightness centroid of ± 25 pixels cross sections along the rough track as the estimated position of the traced flows and its second-order central moment as the measurement error. Finally, in accordance with Byrne et al. (2013), we used a Savitzky-Golay filter (Savitzky and Golay 1964) to smooth the obtained tracks. The smoothed tracks would be used for deriving the velocity of MFs.

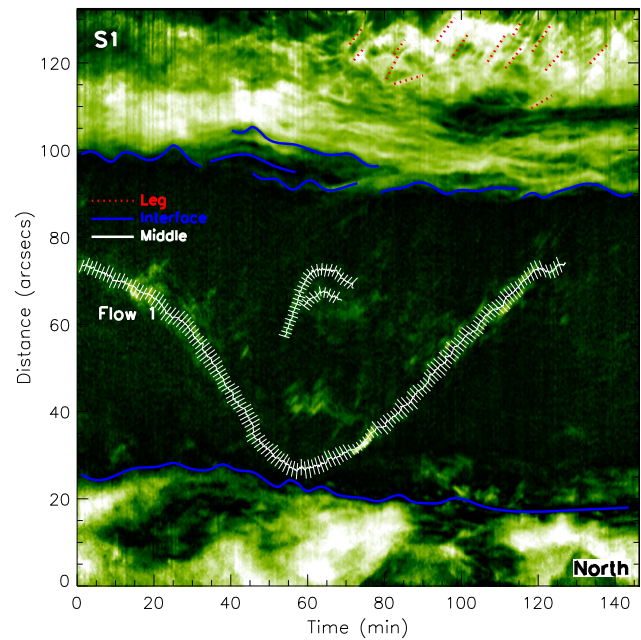


Fig. 2 The time-distance map of S1, which is plotted from its north leg to its south leg. The two types of MFs are indicated as the red dotted and white solid lines. The interfaces between them are indicated by the blue solid lines

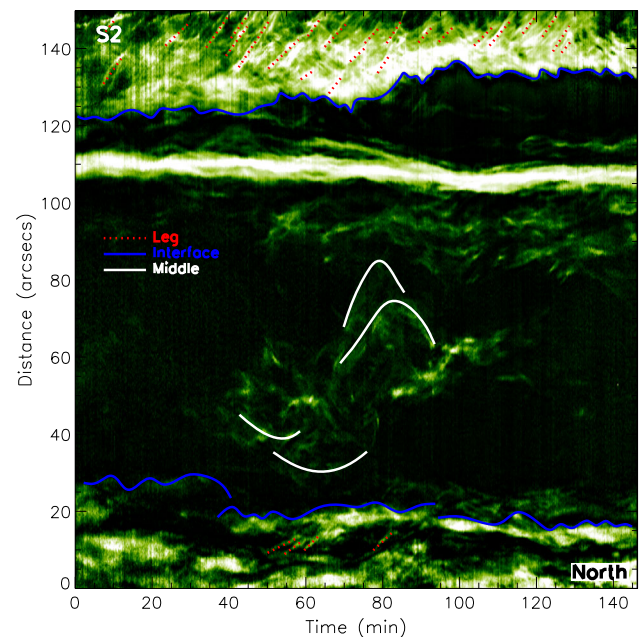


Fig. 3 The time-distance map of S2, where the two types of MFs and the interfaces between the leg and middle section of the prominence are indicated as the red dotted, white solid and blue solid lines, respectively. The upward flows are indicated by the dotted lines at north leg of S2 between 50–90 minutes

3 Results

As it is shown in Fig. 1, the prominence of interest consists of two entwined branches (S1 and S2). The brightness of

them is very inhomogeneous: both branches have two distinct legs that are obviously brighter than the middle section of them. Between the middle section and legs of each branch, a sharp transition region can be identified, through which the brightness of prominence fades sharply toward its middle. The plasma appears to be independent in each part of prominence, which implies that the prominence could be subdivided into different parts with distinct physical properties.

Similar with the radiation, the MFs on the prominence have also distinctly different behaviors. From the time-distance maps of S1 and S2 (Fig. 2 and Fig. 3), we can clearly identify two main types of MFs. One type of MFs is the circular flow that keeps flowing in a particular region and changes its direction near the prominence legs. It seems to be that the material is trapped in the middle section of the prominence. The other one is the apparently downward flow of 14.3 ± 3.5 km/s in the prominence south leg. All of these are further confirmed that the prominence should have different conditions between its middle section and legs. Moreover, we have also noticed that there are some upward flows near the north leg of S2 highlighted as dotted lines in Fig. 3. They have an average speed of 9.5 ± 2.6 km/s, but only appear in a very short time interval (about 40 of 146 min) during our observation. Finally, it should be noticed that the bright ribbon in the up middle of Fig. 3 is just the projection of S1.

4 Discussion and conclusion

Prominences, as the main magnetic structures in solar atmosphere, are important for understanding both solar eruptions and our terrestrial space weather (Lin and Forbes 2000; Liu et al. 2014a, 2016; Schmieder et al. 2008; Yang et al. 2014; Li and Zhang 2015; Schmieder et al. 2015; Li et al. 2016; Wang et al. 2016; 2017; Xue et al. 2016). Previous studies have revealed that many prominences have a fairly uneven distribution of radiation (Lin et al. 2005; Martin 2015; Shen et al. 2015). Their legs are much brighter than their middle sections, which implies that it should have different physical properties between the leg and middle section of them. In addition, observations also reveal that the material inside the prominence is not stillness (Zirker et al. 1998; Ning et al. 2009; Yang et al. 2014; Okamoto et al. 2016). In fact, the material of prominence is highly dynamic. It can move and form MFs within prominences (Mackay et al. 2010). There are a variety of MFs observed in many previous works (Berger et al. 2011; Li and Zhang 2013; Chen et al. 2014; Shen et al. 2014; Yang et al. 2014; Zhang et al. 2014; Shen et al. 2015). However, the work with different types of MFs observed in the same prominence simultaneously was rarely reported.

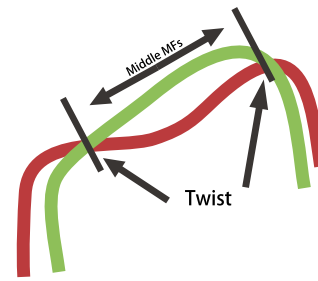


Fig. 4 A schematic model demonstrating the magnetic structure of the prominence. The green and red lines represent the entwined branches, which constitute the prominence. Two twisted knots are indicated by the two black arrows, between which the middle MFs can be identified

In this work, we present a prominence that have two bright legs and a tenuous middle section. It shows that the MFs in the middle section and legs of this prominence have distinctly different performances: (1) the material in the middle section of the prominence is mainly restricted to flow back and forth at a certain region, while the material in the leg of the prominence primarily drops into the photosphere; (2) obvious interfaces can be identified between the middle section and legs of the prominence; and (3) there are some upward flows near the north interface of the prominence branch S1. Since the mass of prominences moves along magnetic field lines, the observed different types of MFs demonstrate that the magnetic field of the studied prominence should be horizontal and vertical at its middle section and legs, respectively, which is consistent with the magnetic flux rope model of prominences (van Ballegooijen and Martens 1989; Li and Zhang 2013, 2015; Xia et al. 2014).

Based on this model and the observed twisted structure of S1 and S2, we propose that the mass may be restrict to the elongated magnetic dips in the middle section of the prominence and flow back and forth because of the gravity (see Fig. 4). According to this, the velocity of circular MFs within the prominence middle should provide information about the longitudinal magnetic structure of the prominence middle. We then traced a complete MF (Flow 1) within S1 by using the method described in Sect. 2. The result is shown in Fig. 5, where the track of Flow 1 and the distribution of its velocity are plotted on the top panels. From the distribution of parallel velocity (top-right panel of Fig. 5), we can see the peak velocity significantly decay during the observation, which directly affects the detection of the prominence magnetic structure. Therefore, we try to normalize the distribution of velocity by an exponential trend that is estimated from the fitting of two velocity peaks. The result indicates that both the original and corrected distributions (Fig. 5, bottom panels) have a clear shift (17 and 19 arcsec, respectively) of their velocity peaks that suggests a shift of the dip bottom. It should be noted that we just do a rough correction for the decay effect because it just has a slight influence on our conclusions. Moreover, we have also investigated the

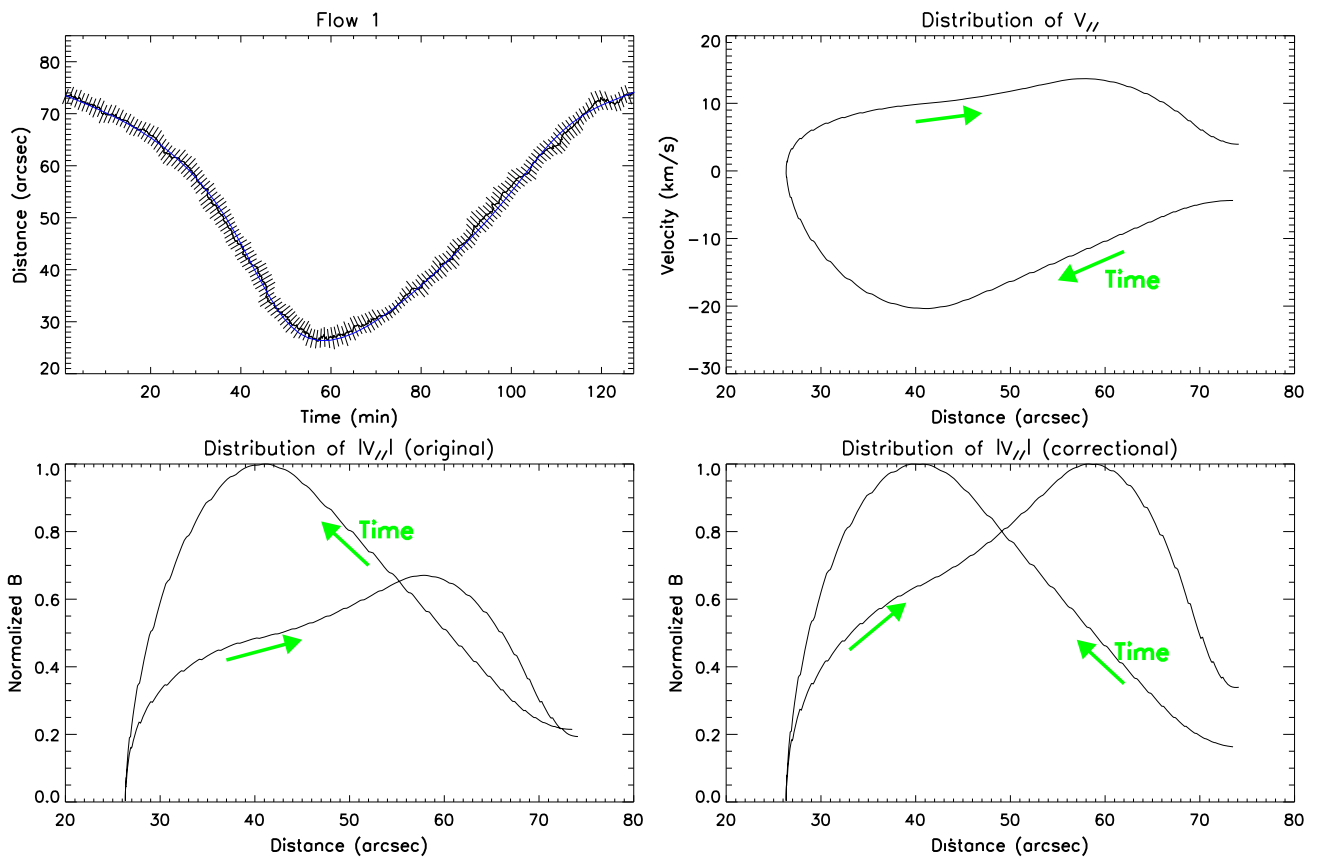
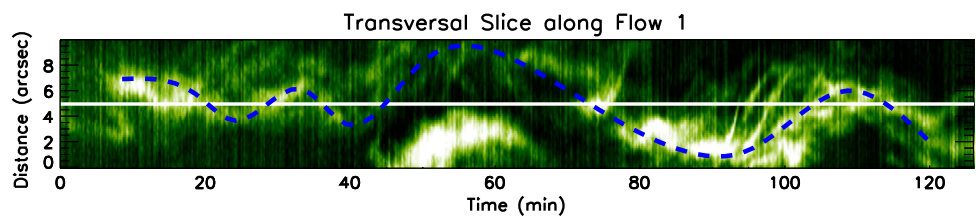


Fig. 5 The analysis results of Flow 1. The Flow 1 is shown in the top-left panel, where original and smooth tracks are plotted as the black and blue curves, respectively. The distribution of parallel velocity is

demonstrated in the top-right panel. The original (left) and corrected (right) distributions of absolute value of parallel velocity are shown in the bottom panels. The direction of time is marked by the green arrows

Fig. 6 The transversal slice along Flow 1, where the main axis of S1 and the track of Flow 1 are plotted as the white solid and blue dashed lines, respectively



transversal slice (Fig. 6) along Flow 1. From Fig. 6, we can find the flow has a slight displacement from the main axis of S1. Both the characteristics indicate that the prominence suffered a slight deformation during Flow 1. Since there is no other disturbance source during the observation, we suggest that the deformation should be caused by the MFs within the prominence.

In addition, it is worth noting that both radiation and MF exhibit distinct characteristics between the middle section and legs of the observed prominence, which may imply some association between this two aspects. The different radiation can be explained as the legs of the prominence are denser than its middle part (Mackay et al. 2010; Parenti 2014; Martin 2015). It is reasonable that the denser plasma is more liable to drop into photosphere and the

rarefied plasma is easier to be trapped in the middle section of the prominence. However, theories regarding to different types of MFs within different parts of prominences are rarely discussed. To better understand the inner structure and dynamics of prominences, realistic models with piecewise radiation and MFs should be developed.

In summary, we present a prominence that with different radiation and MFs between its legs and middle section. It suggests that the different MFs may caused by the different oriented magnetic field and inhomogeneous physical conditions of the prominence. Besides, we also analyze the velocity distribution of a circular MF within the prominence middle. The result indicates that the prominence could be slightly deformed by the MFs within it. Nevertheless, this

study shows us an interesting observation of MFs, which may shed some light on the inner of the prominence. For more details about the different MFs within different parts of prominence, further observations and investigations are worth to be performed.

Acknowledgements The authors are deeply indebted the anonymous referee for his/her constructive advices and corrections. We are grateful for the observation provided by the NVST. We also thank Dr. K. Ji and J. Su for their help. This work is supported by Grants from National Scientific Foundation of China (NSFC 11533009, 11603074, 11503084, 11773068) and from the Key Laboratory of Geospace Environment, CAS, University of Science & Technology of China. K.V.T. is supported by Macao Science and Technology Development Fund (FDCT-16-003-SSI). This work is also supported by the grant associated with project of the Group for Innovation of Yunnan Province. Finally, we are also grateful to the One belt and One road project of the West Light Foundation, CAS.

References

- Berger, T.E., Shine, R.A., Slater, G.L., et al.: *Astrophys. J. Lett.* **676**, L89 (2008)
- Berger, T.E., Testa, P., Hillier, A., et al.: *Nature* **472**, 197 (2011)
- Byrne, J.P., Long, D.M., Gallagher, P.T., et al.: *Astron. Astrophys.* **557**, A96 (2013)
- Chen, P.F., Harra, L.K., Fang, C.: *Astrophys. J.* **784**, 50 (2014)
- Hirayama, T.: *Sol. Phys.* **100**, 415 (1985)
- Li, T., Zhang, J.: *Astrophys. J. Lett.* **770**, L25 (2013)
- Li, T., Zhang, J.: *Sol. Phys.* **290**, 2857 (2015)
- Li, H., Liu, Y., Elmhamdi, A., Kordi, A.-S.: *Astrophys. J.* **830**, 132 (2016)
- Lin, Y.: *Space Sci. Rev.* **158**, 237 (2011)
- Lin, J., Forbes, T.G.: *J. Geophys. Res.* **105**, 2375 (2000)
- Lin, Y., Engvold, O., Wiik, J.E.: *Sol. Phys.* **216**, 109 (2003)
- Lin, Y., Engvold, O., Ruppe van der Voort, L., Wiik, J.E., Berger, T.E.: *Sol. Phys.* **226**, 239 (2005)
- Liu, Y., Kurokawa, H.: *Publ. Astron. Soc. Jpn.* **56**, 497 (2004)
- Liu, Y.D., Luhmann, J.G., Kajdič, P., et al.: *Nat. Commun.* **5**, 3481 (2014a)
- Liu, Z., Xu, J., Gu, B.Z., et al.: *Res. Astron. Astrophys.* **14**, 705 (2014b)
- Liu, R., Kliem, B., Trtov, V.S., et al.: *Astrophys. J.* **818**, 148 (2016)
- Mackay, D.H., Karpen, J.T., Bellester, J.L., Schmieder, B., Aulanier, G.: *Space Sci. Rev.* **151**, 333 (2010)
- Martin, S.F.: *Sol. Phys.* **182**, 107 (1998)
- Martin, S.F.: *Solar Prominences* **415**, 205 (2015)
- Ning, Z., Cao, W., Okamoto, T.J., Ichimoto, K., Qu, Z.Q.: *Astron. Astrophys.* **499**, 595 (2009)
- Okamoto, T.J., Liu, W., Tsuneta, S.: *Astrophys. J.* **831**, 126 (2016)
- Parenti, S.: *Living Rev. Sol. Phys.* **11**, 1 (2014)
- Savitzky, A., Golay, M.: *Anal. Chem.* **36**, 1627 (1964)
- Schmieder, B., Bommier, V., Kitai, R., et al.: *Sol. Phys.* **247**, 321 (2008)
- Schmieder, B., Chandra, R., Berlicki, A., Mein, P.: *Astron. Astrophys.* **514**, A68 (2010)
- Schmieder, B., Aulanier, G., Vršnak, B.: *Sol. Phys.* **290**, 3457 (2015)
- Shen, Y., Liu, Y.D., Chen, P.F., Ichimoto, K.: *Astrophys. J.* **795**, 130 (2014)
- Shen, Y., Liu, Y., Liu, Y.D., et al.: *Astrophys. J. Lett.* **814**, L17 (2015)
- Su, Y., van Ballegooijen, A., McCauley, P., et al.: *Astrophys. J.* **807**, 144 (2015)
- van Ballegooijen, A.A., Martens, P.C.H.: *Astrophys. J.* **343**, 971 (1989)
- Wang, J., Yan, X., Qu, Z., et al.: *Astrophys. J.* **817**, 156 (2016)
- Wang, J., Yan, X., Qu, Z., et al.: *Astrophys. J.* **839**, 128 (2017)
- Xia, C., Keppens, R., Guo, Y.: *Astrophys. J.* **780**, 130 (2014)
- Xiang, Y.-y., Liu, Z., Jin, Z.-y.: *New Astron.* **49**, 8 (2016)
- Xue, Z., Yan, X., Cheng, X., et al.: *Nat. Commun.* **7**, 11837 (2016)
- Yan, X.L., Xue, Z.K., Xiang, Y.Y., Yang, L.H.: *Res. Astron. Astrophys.* **15**, 1725 (2015)
- Yang, S., Zhang, J., Liu, Z., Xiang, Y.: *Astrophys. J. Lett.* **784**, L36 (2014)
- Zhang, Q., Liu, R., Wang, Y., et al.: *Astrophys. J.* **789**, 133 (2014)
- Zirker, J.B., Engvold, O., Martin, S.F.: *Nature* **396**, 440 (1998)